NRL Memorandum Report 5777

The VIPER Conductivity Model

S. P. SLINKER AND R. F. HUBBARD

Plasma Theory Branch
Plasma Physics Division

April 24, 1986

This work was supported by the Defense Advanced Research Projects Agency under ARPA Order No. 4395, Amendment No. 54, and monitored by the Naval Surface Weapons Center under Contract No. N60921-85-WR-W0239.

NAVAL RESEARCH LABORATORY
Washington, D.C.

SECURITY CLASSIFICATION OF THIS PAGE

REPORT DOCUMENTATION PAGE

1a. REPORT SECURITY CLASSIFICATION UNCLASSIFIED	1b. RESTRICTIVE MARKINGS
2a. SECURITY CLASSIFICATION AUTHORITY	3. DISTRIBUTION / AVAILABILITY OF REPORT Approved for public release; distribution unlimited.
2b. DECLASSIFICATION / DOWNGRADING SCHEDULE	
4. PERFORMING ORGANIZATION REPORT NUMBER(S) NRL Memorandum Report 5777	5. MONITORING ORGANIZATION REPORT NUMBER(S)
6a. NAME OF PERFORMING ORGANIZATION Naval Research Laboratory 6b. OFFICE SYMBOL (If applicable) Code 4790	7a. NAME OF MONITORING ORGANIZATION Naval Surface Weapons Center
6c. ADDRESS (City, State, and ZIP Code) Washington, DC 20375-5000	7b. ADDRESS (City, State, and ZIP Code) Silver Spring, MD 20910
8a. NAME OF FUNDING / SPONSORING ORGANIZATION DARPA 8b. OFFICE SYMBOL (If applicable)	9. PROCUREMENT INSTRUMENT IDENTIFICATION NUMBER
8c. ADDRESS (City, State, and ZIP Code) Arlington, VA 22209	10. SOURCE OF FUNDING NUMBERS PROGRAM ELEMENT NO. 62707E; PROJECT NO.; TASK NO.; WORK UNIT ACCESSION NO. DN680-415

11. TITLE (Include Security Classification)
The VIPER Conductivity Model

12. PERSONAL AUTHOR(S)
Slinker, S. P. and Hubbard, R. F.

13a. TYPE OF REPORT	13b. TIME COVERED	14. DATE OF REPORT (Year, Month, Day)	15. PAGE COUNT
Interim	FROM _____ TO _____	1986 April 24	21

16. SUPPLEMENTARY NOTATION This work was supported by the Defense Advanced Research Projects Agency under ARPA Order No. 4395, Amendment No. 54, and monitored by the Naval Surface Weapons Center under Contract No. N60921-85-WR-W0239.

17. COSATI CODES		
FIELD	GROUP	SUB-GROUP

18. SUBJECT TERMS (Continue on reverse if necessary and identify by block number)
Air chemistry; Beam generated ionization; Beam propagation; Beam generated conductivity; Charged particle beam; Intense relativistic electron beam

19. ABSTRACT (Continue on reverse if necessary and identify by block number)

Beam propagation codes such as the hose simulation code VIPER require simple models for treating the generation of conductivity by the beam pulse. The VIPER conductivity model calculates the electron density $n_e(r,\zeta,z)$ where $\zeta = ct-z$ is the distance from the beam head. The rate equation for n_e treates beam impact ionization, avalanche ionization, and recombination. Rate coefficients and momentum transfer frequency are functions of the electron temperature T_e which is itself estimated from the ratio of the local electric field to the neutral gas density. Since VIPER treats both monopole and dipole beam dynamics, the perturbed or dipole conductivity must also be calculated. Benchmark comparisons between the VIPER model and more elaborate treatments of beam-generated conductivity are also presented.

Keywords:

20. DISTRIBUTION / AVAILABILITY OF ABSTRACT ☒ UNCLASSIFIED/UNLIMITED ☐ SAME AS RPT. ☐ DTIC USERS	21. ABSTRACT SECURITY CLASSIFICATION UNCLASSIFIED
22a. NAME OF RESPONSIBLE INDIVIDUAL S. P. Slinker	22b. TELEPHONE (Include Area Code) (202) 767-3720 22c. OFFICE SYMBOL Code 4790

DD FORM 1473, 84 MAR 83 APR edition may be used until exhausted. All other editions are obsolete.

SECURITY CLASSIFICATION OF THIS PAGE

CONTENTS

INTRODUCTION 1

BEAM PRODUCTION 2

AVALANCHE IONIZATION 3

RECOMBINATION 5

ATTACHMENT 6

COLLISION FREQUENCIES 6

ELECTRON TEMPERATURE 7

SUMMARY OF MONOPOLE AND DIPOLE EQUATIONS 9

NUMERICAL CONSIDERATIONS 11

BENCHMARK 11

CONCLUSIONS 13

ACKNOWLEDGMENT 13

REFERENCES 16

The VIPER Conductivity Model

INTRODUCTION

In this paper we briefly discuss the conductivity models used in the electron beam propagation code VIPER[1]. This is a linearized code built to study the resistive hose instability in an electron beam propagating in air. The beam ionizes the air creating a plasma whose conductivity modifies the beam generated fields. VIPER uses the ultrarelativistic frozen approximation, replacing z and t by z (the position in the lab frame) and $\zeta = ct-z$ (the distance from the beam head). In a typical run there may be 200 beam slices, each slice having 50 radial points at which the conductivity must be calculated. These slices move ~ 400 steps in space. In addition, the perturbed or dipole conductivity must be found at all the points.

A complete calculation of the conductivity is extremely difficult[2]. Dozens of species of neutrals, ions and their excited states are created. They react with the beam, the plasma electrons, and themselves. In many cases the reaction rates are not known or there is inconsistent experimental evidence for them. The plasma electrons are mobile and are affected by the electric and magnetic fields of the beam. In addition, chemical reaction systems are notoriously stiff numerically. Computational models which offer a comprehensive treatment of air chemistry and conductivity generation, such as CHMAIR[3], ETWAC[4], NUTS[5], and HICHEM[6], treat the beam at one z-position in space. It is clearly impossible to put this much detail into the propagation code, which typically requires several hundred z-steps, and expect to do any

Manuscript approved February 26, 1986.

kind of parametric study. Therefore some of the details of a complete air chemistry description must be compromised. The VIPER model attempts to describe the major processes affecting propagation of a beam similar to the ATA beam entering the atmosphere in a way which is fast enough numerically to be useful.

The VIPER chemistry model is similar in structure and complexity to those used in the EMPULSE[7] and PHLAP[8] propagation codes. This model has been incorporated into other NRL propagation codes such as SIMM0, SIMM1, and SARLAC[9-11]. In these codes, both chemistry and field equations involve only derivatives in ζ. The VIPER model contains monopole and dipole rate equations for $n_e(r,\zeta)$, an empirical relation for calculating T_e as a function of E/P, model equations for rate coefficients and momentum transfer frequency ν_m as functions of T_e, and the usual definition $\sigma = n_e e^2/m\nu_m$. The original VIPER model, which assumes constant ν_m, is still used on some occasions.

BEAM PRODUCTION

The beams of interest have energies in the MeV range. When the beam enters a gas it ionizes the molecules, atoms and ions present. The energetic secondaries created in these collisions, in turn, produce further ionization and energy deposition. If the mean free path is small, the secondaries cascade down in energy near the point in space where they were born. This is an assumption made in the VIPER model: beam ionization and the associated cascade is local and instantaneous. This is a good approximation in 760 torr air and is probably acceptable down to ~ 100 torr[12]. Below that nonlocal effects begin to be seen[6,12]. Thus beam ionization or direct production is modeled by

$$\frac{dn_e}{dt} = sPJ_b \qquad (1)$$

where s is a constant direct production coefficient (during a given run), P is ratio of the background density to that of a standard atmosphere, and J_b is the current density of the beam. s can be written as

$$s = (d\varepsilon/dx)/(W) \qquad (2)$$

where $d\varepsilon/dx$ is the stopping power in a standard atmosphere and W is the average energy needed to create an electron-ion pair. Both of these quantities depend weakly on the beam energy and the atmospheric specie concentration. In molecular and atomic nitrogen and oxygen $d\varepsilon/dx$ rises from roughly 2200 eV/cm for 1 MeV beam electrons to ~ 3000 eV/cm for 100 MeV beam electrons[13]. Though this variation is small it is important to keep in mind when comparing predictions for different accelerators. Below 1 MeV the energy loss increases rapidly. The energy per ion pair is around 35 eV for the gases found in distrubed air[14]. The VIPER value used for ATA (beam energy 50 MeV) is:

$$dn_e/dt\ [1/cm^3 - sec] = 5.4 \times 10^{20} P J_b\ [amps/cm^2] \qquad (3)$$

which corresponds to $(d\varepsilon/dx)/(DW) = 86.4\ [1/cm]$.

Direct production is usually the major conductivity production effect and it is important throughout the pulse.

AVALANCHE IONIZATION

A high current, fast rising beam produces large electric fields. These fields can cause the plasma electrons to avalanche, producing an exponential growth in the electron density and conductivity which tries to short out the

field. Large radial electric fields occur in the nose before the beam is charged neutralized. A large inductive axial field occurs on axis if the current rise time is short. As the pressure is lowered the threshold for avalanche is easier to achieve.

It has been shown that the hollowing instability can be excited by avalanche[9]. The VIPER code, because it uses an envelope model, cannot study the hollowing instability.

The contribution to the electron density due to avalanche is given by

$$dn_e/dt = \alpha(E/P)n_e \qquad (4)$$

where α is the avalanche coefficient and E/P is the magnitude of the electric field divided by the pressure. The expression for α is found in Ali[15],

$$\alpha/P = \begin{cases} [5\times10^{+7} + 0.21\times10^{7}(\frac{E}{P})] \exp(-273.8/(E/P)) & \text{for } 50 < E/P < 120 \text{ v/cm/torr} \\ 4.97\times10^{7}(\frac{E}{P})^{1/2} \exp(-359/(E/P)) & \text{for } E/P > 120 \text{ v/cm/torr} \end{cases} \qquad (5)$$

This expression agrees with the Felsenthal and Proud model used in RINGBEARER[16] and in the original VIPER chemistry model for moderate values of E/P and is lower beyond that. The reason for the differences are given in (15).

In most beams where avalanche ionization is important, hose growth tends to be more violent because high E/P values lead to a reduction in ν_m, the momentum transfer frequency. If avalanche is strong enough to excite the hollowing instability[9], the resulting peaking of return current flow on axis is strongly destabilizing for hose as well. Thus, most VIPER simulations are performed using parameters which result in negligible avalanche ionization.

RECOMBINATION

Dissociative recombination is the main sink for electrons in disturbed air. The contribution to the electron density is

$$dn_e/dt = -\beta n_e^2 \qquad (6)$$

where β is the effective recombination coefficient.

Recombination is not important in the nose of the beam where the electron density is low. In the tail, however, it balances off the direct production of the beam and the electron density becomes nearly constant.

Recombination helps to stabilize the hose[17], because, although it limits the amount of conductivity, it broadens the radial profile of the conductivity and the plasma current. Plasma current flowing outside the beam has a strong stabilizing effect on hose.

Recombination rates are strongly dependent on the type of molecular ion present. It can vary by two orders of magnitude for one volt electrons. In dry air the predominant ions early in the pulse are N_2^+ and O_2^+. These react and produce many cluster ions later in the pulse. The cluster ions have faster recombination rates. For very long times NO^+ dominates. If water vapor is present the effective recombination rate is large because of the hydrated clusters which form[4]. Complicating this is the fact that many of the rates are not well verified experimentally.

The recombination rate coefficient used in VIPER is

$$\beta = 0.6\beta(N_2^+) + 0.4\beta(O_2^+) \qquad (7)$$

where $\beta(N_2^+) = \frac{4.33\times10^{-8}}{T_e^{0.39}}$ is the coefficient for $N2^+$ and $\beta(O_2^+) = \frac{2.1\times10^{-8}}{T_e^{0.56}}$ is that for O_2^+ [13]. This combination was chosen to fit more sophisticated air chemistry modelling results for fast rising beams like ATA in dry air[15].

In summary, recombination must be included if the beam is over a few nanoseconds long. It is very dependent on the beam parameters and the composition of the background. Many of the rates are not well measured. A constant rate is probably acceptable, but if temperature dependence is included, the rate should decrease slowly as the temperature rises.

ATTACHMENT

Oxygen readily attaches low energy electrons. Attachment primarily occurs in the wings and tail of a beam. It is a three body process so it becomes less important as the density decreases. Attachment is not included in the VIPER model.

COLLISION FREQUENCIES

The electron-neutral collision frequency, ν_{en}, comes from a polynomial fit to rates computed for a Maxwellian electron distribution[18] using a recent compilation of the momentum transfer cross sections for nitrogen and oxygen[19]. The fit is given by

$$\frac{\nu_{en}}{D} = \begin{cases} 6.3966\times10^{-9} + 1.6629\times10^{-7}T_e - 2.6852\times10^{-8}\,T_e^2 + 2.5504\times10^{-9}T_e^3 & T_e < 5 \text{ eV} \\ 1.1158\times10^{-7} + 1.7366\times10^{-8}T_e - 4.8897\times10^{-10}\,T_e^2 & T_e > 5 \text{ eV} \end{cases} \tag{8}$$

where D is the neutral density in cm^{-3}. Figure 1 shows the polynomial fit for ν_{en}/D and the computed rates. Since $T_e \leq 2$ eV in most cases of interest, the polynomial fit is quite accurate.

The electron-ion collision frequency, ν_{ei}, is given by[20]

$$\nu_{ei} = \frac{4}{3}\frac{\sqrt{2\pi}}{m} e^4 \frac{\ell n\lambda}{T_e^{3/2}} n_e. \qquad (9)$$

The electron-ion contribution is negligible in the nose. For long beams, the ion density can become large enough so that the electron-ion term can become comparable to, or even surpass the electron-neutral term. In the current model $\ell n\lambda$ is held fixed, although for long pulse beams its variation should be considered.

The total collision frequency is simply taken to be the sum of the electron-neutral and electron-ion terms. This is a good approximation when one of them dominates. The proper weighting requires a knowledge of the electron distribution function[2].

The conductivity is then given by

$$\sigma = \frac{e^2}{m} \frac{n_e}{(\nu_{en} + \nu_{ei})}. \qquad (10)$$

It has been shown that inclusion of a temperature (or E/P) dependence in the collision frequency results in a new destabilizing term to the dipole conductivity. When compared with a fixed ν_m conductivity model an "E/P" model usually gives more growth in the beam head, but reduced local growth rates in the beam tail[21].

ELECTRON TEMPERATURE

It is assumed that the plasma sea of electrons are Maxwellian, or at least can be characterized by an electron temperature. There are many processes that contribute to the determination of this temperature. The major

heating processes are direct beam heating and ohmic deposition. The electrons which enter the plasma after they cascade down in energy from their creation in the beam ionization process mentioned above, are assumed to be "born" with an energy of about 7.5 eV. This source of energy continues as long as the beam is on and is the dominant heating source in the body. Ohmic heating, which is proportional to the square of the total electric field, makes a significant contribution in the nose. The electrons are cooled by their interactions with the background gas. The major source of cooling is the excitation of the vibrational levels of nitrogen. These have a large cross section for collisions with low energy electrons.

Rather than try to solve a rate equation for the electron temperature, the VIPER model uses an analytic relation between the local electric field and the temperature

$$T_e = 0.1 \left(\frac{E}{P}\right)^{0.8} + T_o \qquad E/P \text{ in volts/cm/torr.} \qquad (11)$$

The first term comes from an analysis of ionization rates by Ali[15]. It reflects a balance between ohmic heating and excitation cooling. T_o is a constant which models the beam heating component. It is set at 0.15 eV for ATA type beams at full density. For lower pressure or for more intense beams a higher value, typically .30 - .35 eV, is used.

In some versions a relation is used which was found from a fit to results from the air chemistry code CHMAIR II[22]

$$T_e = 0.20 + 0.313 \left(\frac{E}{P}\right)^{1/2} + 0.0174 \frac{E}{P} \qquad \frac{E}{P} \text{ in kv/cm/atm.} \qquad (12)$$

The $T_e(E/P)$ relationship is most accurate in regions of the beam where ohmic heating is the dominant heating mechanism. Thus, it is well-suited for treating the beam head and body where most hose growth usually occurs. It is less accurate for the tail region of long pulses where collisional beam deposition can be the dominant heating mechanism.

SUMMARY OF MONOPOLE AND DIPOLE EQUATIONS

The results from the previous sections are combined to give rate equations for the monopole and dipole electron densities $n_e(r,\zeta)$ and $\hat{n}_e(r,\zeta)$. Replacing the time derivatives in (3), (4), and (6) with $c\frac{\partial}{\partial\zeta}$ gives

$$c\frac{dn_e}{d\zeta} = sPJ_b + \alpha(E/P)n_e - \beta(T_e)n_e^2 \qquad (13)$$

the rates s, α, and β are given in (3), (5), and (7) respectively. The conductivity $\sigma(n_e,T_e)$ is given in (10), using the collision frequencies in (8) and (9). The temperature T_e is taken from the E/P relations in (11) or (12). The monopole conductivity equations are used to give $\sigma(r,\zeta)$ in VIPER, SIMM0, and SIMM1 and $\sigma(r,\zeta,\theta)$ in the SARLAC model.

Linearized hose codes such as VIPER and SIMM1 require equations for the dipole or perturbed conductivity. Additional terms appear for the temperature dependent rate coefficients. Using "^" to denote dipole quantities, we have

$$c\frac{d\hat{n}_e}{d\zeta} = sP\hat{J} + \alpha\hat{n}_e - \hat{\alpha}n_e - \beta\hat{n}_e^2 - 2\beta n_e\hat{n}_e, \qquad (14)$$

and

$$\hat{\sigma} = \frac{e^2}{m}\frac{\hat{n}}{\nu_m} - \sigma\frac{\hat{\nu}_m}{\nu_m}. \qquad (15)$$

Since the coefficients α, β, and ν_m are functions of $T_e(E/P)$, the dipole coefficients $\hat{\alpha}$, $\hat{\beta}$, and $\hat{\nu}_m$ are given by appropriate derivatives of these coefficients. For example,

$$\hat{\beta} = \frac{\partial \beta}{\partial T_e} \hat{T}_e = \frac{\partial \beta}{\partial T_e} \frac{\partial T_e}{\partial E} \hat{E}, \tag{16}$$

with the dipole electric field $\hat{E}$ given by

$$\hat{E} = \frac{E_z \hat{E}_z + E_r \hat{E}_r}{(E_z^2 + E_r^2)^{1/2}}. \tag{17}$$

The actual equations used in VIPER employ a set of dimensionless units widely used in the beam propagation community. Using primes to denote dimensionless quantities and scaling to the nominal beam radius a_o, we have

$$\zeta = a_o \zeta' \tag{18a}$$

$$J = \frac{mc^3}{4\pi a_o^2 e} J' \tag{18b}$$

$$\sigma = \frac{c}{4\pi a_o} \sigma' \tag{18c}$$

$$n = \frac{1}{4\pi a_o^2 r_o} n' \tag{18d}$$

$$s = \frac{1}{e a_o} s' \tag{18e}$$

$$\alpha = \frac{c}{a_o} \alpha' \tag{18f}$$

$$\beta = 4\pi c a_o r_o \beta' \tag{18g}$$

$$\nu_m = \frac{c}{a_o} \nu_m' . \qquad (18h)$$

The dimensional quantities are in cgs units, and $r_o = e^2/mc^2$ is the classical electron radius. The dimensionless forms of (10) and (13-15) have c and e^2/m replaced by 1. The detailed diagnostics output from VIPER are in terms of the dimensionless units described above.

NUMERICAL CONSIDERATIONS

The differential equations are solved by a simple differencing. If the avalanching becomes important an integrating factor is automatically used. The conductivity and field solver are advanced by a leapfrog scheme. If the fields change too rapidly or the hose motion becomes too violent an automatic subgridding of the timestep is performed. Although the coefficients are given by analytic formulas, we usually began a run by setting up tables indexed on E/P and use a fast table lookup routine thereafter.

BENCHMARK

Table 1 shows a comparison for some of the air chemistry quantities for similar runs between the VIPER model discussed above and the radially resolved CHMAIR II model[23]. CHMAIR II is a detailed air chemistry code containing many species and reactions. The data are given at the injection point for a beam similar to the ATA beam, 10 kA and 50 MeV. Figure 2 shows the electron temperature plotted versus the electric field at several radii in the CHMAIR run. The VIPER E/P relationship is also shown.

Table 1. Comparison of CHMAIR II and VIPER chemistry. Values are given on-axis

	CHMAIR	VIPER	CHMAIR	VIPER	CHMAIR	VIPER
Time(ns)	1	1	10	10	21.6	20
E_z(v/cm)	5850	5827	1460	1812	1100	876
T_e(eV)	.58	.66	.323	.319	.327	.284
ν_{en}(d'less)	24	28.5	14.8	16.3	15	15
α(d'less)	4.9×10^{-15}	3.0×10^{-16}	2.9×10^{-17}	0	1.66×10^{-16}	0
β(d'less)	7.8×10^{-7}	7.7×10^{-7}	1.26×10^{-6}	1.06×10^{-6}	9.3×10^{-7}	1.1×10^{-6}
σ(d'less)	2.75	2.66	200	233	315	284

CONCLUSIONS

We have presented an air chemistry model which is numerically fast and stable enough to be used in a linearized propagation code. The model is tuned to electron beams comparable to the ATA beam entering dry air. Processes determining the electron density are direct ionization, avalanche ionization, and dissociative recombination. Temperature dependent electron-neutral and electron-ion collision frequencies are included.

ACKNOWLEDGMENT

We are greatly indebted to Dr. A. W. Ali for guidance in all aspects of this endeavor. In addition, we acknowledge many useful discussions on this subject with Drs. G. Joyce and M. Lampe.

This work was supported by the Defense Advanced Research Projects Agency under ARPA Order No. 4395, Amendment No. 54, and monitored by the Naval Surface Weapons Center. A portion of the work was supported by Contract N00014-83-C-2038 with JAYCOR.

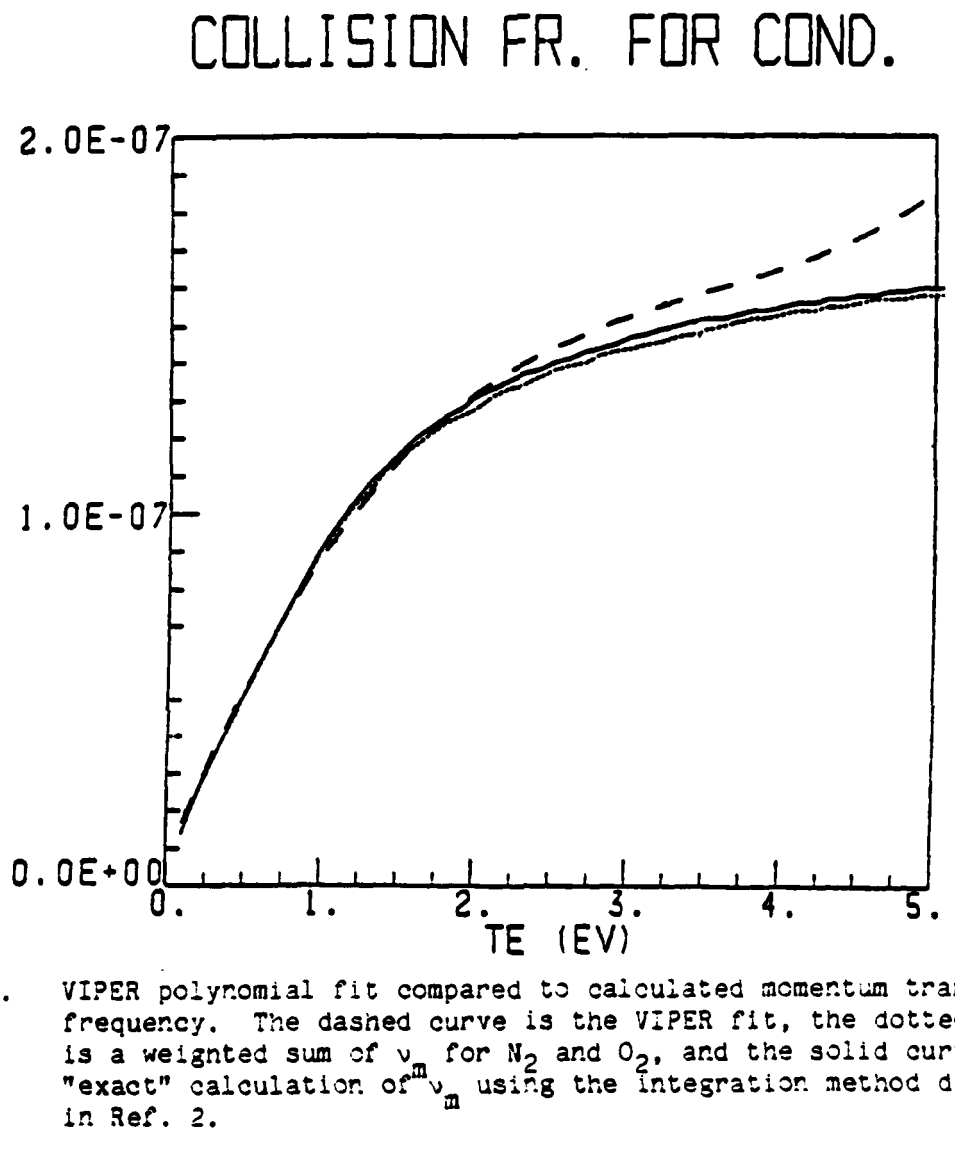

Figure 1. VIPER polynomial fit compared to calculated momentum transfer frequency. The dashed curve is the VIPER fit, the dotted curve is a weighted sum of ν_m for N_2 and O_2, and the solid curve is an "exact" calculation of ν_m using the integration method described in Ref. 2.

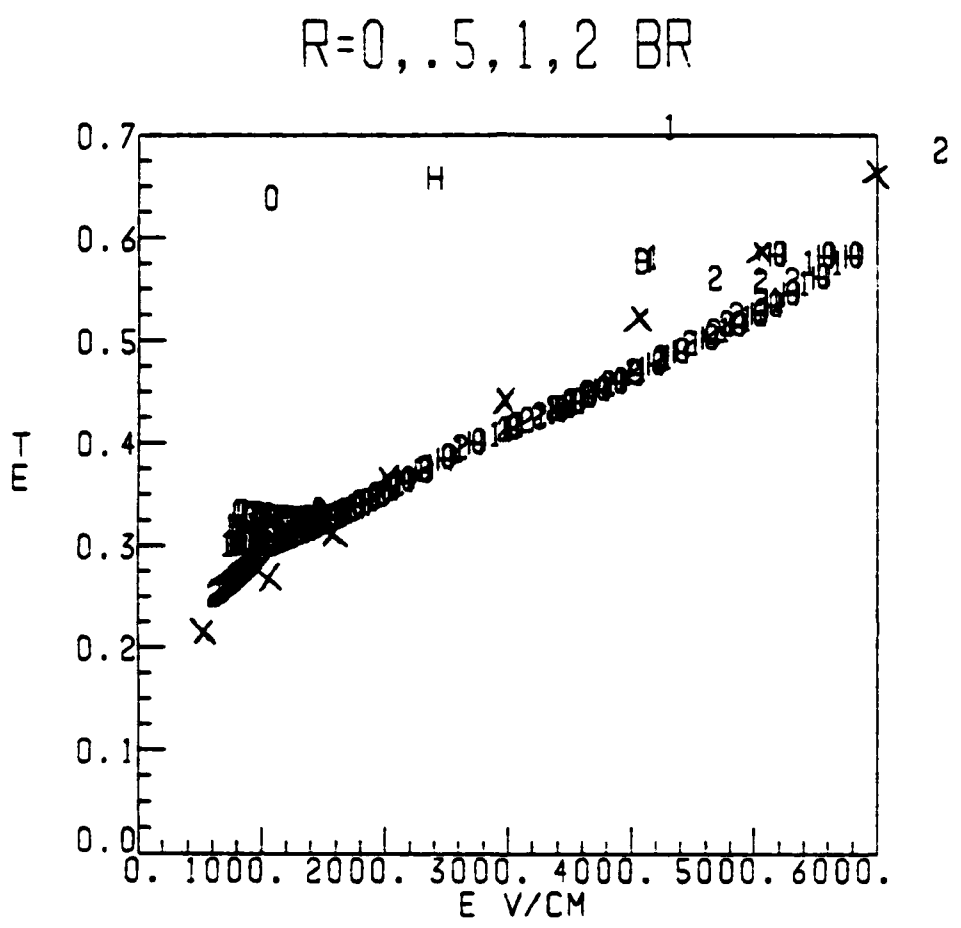

Figure 2. T_e vs. E for CHMAIR run. The data points are taken at r=0, .25, .5 and 1 cm down the beam. The X's are what VIPER would predict.

REFERENCES

1. R. F. Hubbard, M. Lampe, S. P. Slinker and G. Joyce, "VIPER I: A Multi-component Hose Dynamics Code", JAYCOR Tech. Report J207-01-005 (1981); Hubbard et al., "Multicomponent Simulations of the Resistive Hose Instability", JAYCOR Tech. Report J207-82-005 (1982).

2. S. S. Yu, "Boltzmann Approach to Conductivity Calculations", Lawrence Livermore Laboratory Report UCID-17907 (1978).

3. A. W. Ali, private communication.

4. A. W. Ali, "The Physics and the Chemistry of ETWAC Code (An Early Time Wet Air Chemistry Code for Disturbed Air Conductivity Calculations)", NRL Memo Report 4537 (1981). ADA100619

5. S. S. Yu and R. E. Melendez, "Nonlocal Boltzmann Theory of Plasma Channels", Lawrence Livermore Laboratory Report UCID-19731 (1983). N8329055

6. R. Johnston, D. Keeley, C. Yee, private communication.

7. E. P. Lee, F. W. Chambers, L. L. Lodestro and S. S. Yu, in Proceedings of the Second International Conference on High Power Electron and Ion Beam Research and Technology, Cornell Univ., 1977, p. 311; W. Fawley and W. Sharp (private communications).

8. R. L. Feinstein, D. A. Keeley, E. R. Parkinson and W. W. Rienstra, Science Applications International Corp. Report SAIC-U-74-PA-DOE (1984).

9. G. Joyce and M. Lampe, Phys. Fluids 26, 3377 (1983).

10. G. Joyce and M. Lampe, "SIMM1 - A Linearized Particle Code", NRL Memo Report 5488 (1984); to appear in J. Comp. Phys. ADA148627

11. R. F. Hubbard, G. Joyce, S. P. Slinker, M. Lampe and J. M. Picone, Bull. Am. Phys. Soc. 30, 1583 (1984).

12. R. J. Briggs and S. S. Yu, "Modeling Beam Front Dynamics at Low Gas Pressures", Lawrence Livermore Laboratory Report UCID-19399 (1982). N83-27842

13. A. W. Ali, "On Electron Beam Ionization of Air and Chemical Reactions for Distrubed Air Deionization", NRL Memo Report 4619 (1981). ADA104517

14. D. J. Strickland and A. W. Ali, "A Code for the Secondary Electron Energy Distribution in air and Some Applications", NRL Memo Report 4956 (1982). ADA121564

15. A. W. Ali, "The Electron Avalanche Ionization of Air and a Simple Air Chemistry Model", NRL Memo Report 4794 (1982). ADA113501

16. F. W. Chambers, J. A. Masamitsu and E. P. Lee, "Mathematical Models and Illustrative Results for the RINGBEARER II Monopole/Dipole Beam Propagation Code", Lawrence Livermore Laboratory Report UCID-19494 (1982). N83-25583

17. M. Lampe, W. Sharp, R. F. Hubbard, E. P. Lee and R. J. Briggs, Phys. Fluids 27, 2921 (1984).

18. S. P. Slinker and A. W. Ali, "Electron Momentum Transfer Collision Frequency in N_2, O_2 and Air", NRL Memo Report 5614 (1985). ADA157030

19. A. W. Ali, "The Electron Momentum Transfer Cross Sections in N2 and 02", NRL Memo Report 5421 (1984). ADA146097

20. D. L. Book, NRL Plasma Formulary (1983) p. 36.

21. S. Slinker, R. Hubbard, R. Fernsler, A. W. Ali and M. Lampe, "Effects of Temperature-Dependent Conductivity of Hose", contained in NRL Memo Report 5412, Beam Propagation Studies at NRL July 1983 to June 1984, Vol. 2 (1984). ADA148198

22. J. Guillory, R. Hubbard, G. Joyce, S. Slinker, S. Kainer and R. Fernsler, "Electron Temperature Dependence on E/P in Air Ionized by Short-Pulse Electron Beams", JAYCOR Tech. Report J207-81-006 (1981).

23. S. P. Slinker and A. W. Ali, unpublished.